phys. stat. sol. (a) **184**, No. 2, 309–317 (2001)

Electrical Conductivity and Conduction ESR in Incommensurate Phase of Graphite Intercalation Compounds $C_{5n}HNO_3$

A. M. ZIATDINOV[1])

Institute of Chemistry, Far Eastern Branch of the Russian Academy of Sciences, Prospekt 100-letiya, 690022 Vladivostok, Russia

(Received February 11, 2000; in revised form November 24, 2000; accepted December 15, 2000)

Subject classification: 64.70.Rh; 72.80.Jc; S11

Electrical conductivity and conduction ESR (CESR) for graphite intercalation compounds (GICs) with nitric acid $C_{5n}HNO_3$ ($n = 2, 3$) have been measured. In the incommensurate phase of second stage compounds ($210\ K < T < 250\ K$) absence of temperature dependence of the *c*-axis conductivity, but preservation of the "metallic" temperature dependence of the basal plane conductivity, has been found. In the third stage compounds the similar "plateau" is a less marked one. In both stages of GICs investigated at the incommensurate crystallization of intercalate subsystem, the CESR linewidth undergoes a stepwise increase. It was shown that in GICs studied the *c*-axis conductivity is realized by means of a non-band mechanism, which might be the mechanism of transport of free charge carriers along the *c*-axis through the defect-mediated narrow high-conductivity paths (channels).

1. Introduction

Graphite intercalation compounds (GICs) consist of an alternating sequence of n hexagonal graphite monolayers ($n = 1, 2, 3$, is called the "stage index" of the compound) and a monolayer of "guest" (intercalant) atoms or molecules. By intercalating the different chemical species into graphite and varying their concentration, it is possible to change under control the sign and concentration of free charge carriers on carbon layers and, as a consequence, electrical, magnetic and mechanical properties of material [1, 2]. One of the most widely studied properties of GICs is electrical conductivity, due to its three remarkable characteristics in acceptor GICs: 1. high conductivity in the basal plane (σ_a), being comparable in some compounds with the conductivity of Cu at room temperature [1, 3], 2. large value of the ratio of σ_a to the *c*-axis conductivity (σ_a/σ_c), reaching values of $\sim 10^5$ in the most acceptor compounds [1, 4–7], and 3. the "metallic" type of temperature dependence of σ_c in compounds with a small stage index (usually, with $n = 3$) [1, 5–7]. The latter property of electrical conductivity in acceptor GICs is unusual and attracts much attention, as the value of σ_c itself in them is tens of times less than the fundamental Ioffe-Regel-Mott limit [8, 9] which provides a criterion for metals. Besides, the typical value of σ_c at room temperature is between 0.1 and $10\ \Omega^{-1}cm^{-1}$ [1, 4–7], leading to a mean free path of less than 1 Å according to the Drude formula, which is almost one order less than the distance between the nearest neighbor graphite layers on either side of the intercalate layer [1, 2].

At present, there is no conventional theory of the *c*-axis conductivity in acceptor GICs. In the literature, for the explanation of the σ_c peculiarities, including the above-

[1]) Tel./Fax: 7(4232)311655/7(4232)311889; e-mail: chemi@online.ru

mentioned ones, alternative models postulating its band [10–14] or non-band [6, 15–20] origin have been suggested. Therefore, search for and study of new properties of σ_c in acceptor GICs, which clarify its origin, are important steps towards creating a theory of the *c*-axis charge transport in these synthetic metals.

In this paper, we report on results of studies of a formerly unknown property of the *c*-axis conductivity in the second stage GICs with nitric acid, consisting in the absence of its temperature dependence in a structural — incommensurate phase. For comparison, the results of investigation of the third stage GICs with nitric acid are presented. For obtaining the additional information about the nature of σ_c, measurements of σ_a and the conduction ESR (CESR) of the compounds investigated were carried out also. The data on conductivity of GICs investigated have been analyzed within the frameworks of existing theoretical models. The conclusion is made that in the GICs studied the conductivity along the *c*-axis between graphite layers through the intervening intercalate layer is determined by the non-band mechanism, through the defect-mediated narrow high conductivity paths (channels). The model of defect formation in incommensurate phase of the investigated compounds has been proposed, which accounts for the absence of σ_c temperature dependence in this phase.

2. Experimental

The $C_{10}HNO_3$ and $C_{15}HNO_3$ compounds investigated belong to the second and third stage of α-modification of GICs with nitric acid, respectively, with the general formula $C_{5n}HNO_3$ ($n = 1, 2, 3,\ldots$). These compounds have been studied by various physical methods [21–33] and according to the data, in particular below $T_c \sim 250$ K, the quasi-two-dimensional liquid-like layers of nitric acid are ordered and form a quasi-two-dimensional crystal. Layers of HNO_3 may be incommensurate with a carbon net along one of its crystallographic direction and they undergo a "lock-in" phase transition at $T_{l\text{-}i} \sim 210$ K [29].

All HOPG plates required for GIC synthesis (for electrical conductivity and CESR measurements) were cut out of a single bar with σ_a and σ_c being equal to $(1.2 \pm 0.2) \times 10^4$ and $(7.7 \pm 0.5)\ \Omega^{-1}\,\mathrm{cm}^{-1}$, respectively. They were in the shape of rectangular parallelepipeds with the dimensions: width (l) × height (h) × thickness (d), where $h \times l$ is the basal plane area. Accuracy in determining the size of plates was $\sim 5 \times 10^{-4}$ cm.

Synthesis of $C_{10}HNO_3$ and $C_{15}HNO_3$ GICs was carried out in liquid nitric acid with density $\varrho \sim 1.565$ and ~ 1.49 g/cm^3, respectively. The GIC stages were determined by X-ray diffraction. From the numerous investigations we noticed the increasing stage homogeneity of compounds (decrease in admixtures of stages other than basic one) at thermocycling of the samples within the temperature range from 100 to 300 K. Therefore, the samples selected for the examination were previously subjected to multiple thermocycling within the stated temperature range. The thermocycling was ceased after the reproducibility of hysteresis curves of the temperature dependences of CESR linewidth for GICs studied had been reached. Within the limits of the experimental accuracy, X-ray measurements of such compounds have shown the absence of admixtures of other stages than basic. The measurements on different samples of a given stage, previously subjected to thermocycling, provide identical results.

The measurements of σ_a of GICs $C_{5n}HNO_3$ ($n = 2, 3$) have been carried out by the contactless Wien bridge method being analogous to that described in Ref. [34].

The measurements of σ_c of GICs investigated have been carried out also by a contactless method in using a CESR technique and the procedure suggested by Saint Jean and McRae [35]. The essence of this method of conductivity determination is as follows. According to Kodera [36] nomograms calculated on the basis of the Dyson expression [37] for CESR line shape in isotropic metals, in the interval $L/\delta < 2$ (L is the sample size, δ is the skin depth, which is determined by the sample conductivity σ) the asymmetry parameter of the first derivative of CESR absorption line, A/B (which is determined as the ratio of the maximum peak height A to the minimum peak height B, both measured with respect to the base line of the resonance derivative) does not depend on spin carrier mobility (Fig. 1). The GICs are two-dimensional metals and in the microwave field of a given configuration the plate regions adjacent to all its vertical faces, i.e. ($h \times l$) and ($h \times d$), situated approximately within the corresponding skin depths, contribute to the CESR [31, 35, 38]. However, in acceptor GICs one may neglect the contribution to CESR from regions adjacent to the basal planes ($h \times l$) due to their high conduction anisotropy ($\sim 10^5$) [31, 35]. As was shown in detail in [31, 35, 39], this peculiarity of acceptor GICs allows analyzing the CESR line shape using the one-dimensional Dyson expression [37] in isotropic metals with $\sigma = \sigma_c$. The latter result enables one to determine the value of δ_c and, consequently, the value of σ_c, for acceptor GICs unambiguously, by measuring the value of A/B for samples with $l/\delta_c < 2$ and using the nomograms in Fig. 1, which were calculated by the author using the Dyson [37] expression for CESR line shape for isotropic metals.

For an estimation of the conduction electron relaxation time in different phases of GICs investigated in CESR-experiments aimed at determination of σ_c (using the narrow samples with $l \sim 2\delta_c$), the value of CESR signal linewidth was simultaneously fixed.

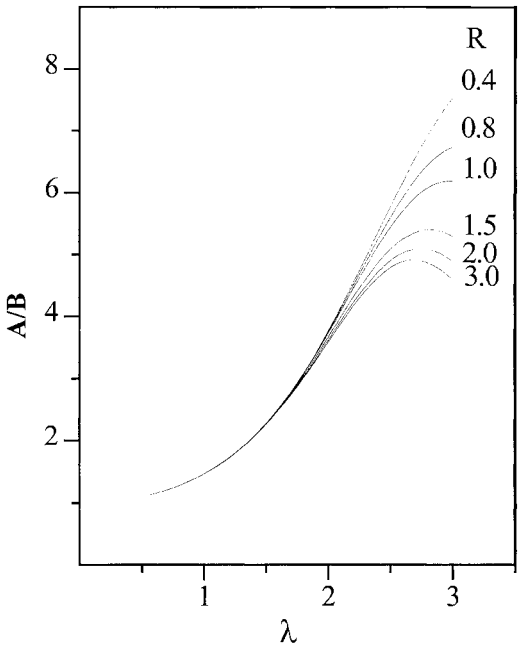

Fig. 1. Theoretical curves of the lineshape asymmetry parameter A/B for the first derivative of CESR absorption line (which is determined as the ratio of the maximum peak height A to the minimum peak height B, both measured with respect to the baseline of the resonance derivative), which were calculated using the Dyson [37] expression for CESR line shape for isotropic metals, versus $\lambda = L/\delta$ (L is the sample size, δ is the skin depth) for different values of parameter $R = (T_D/T_2)^{1/2}$ (T_D is the in-plane spin diffusion time across the skin depth δ, and T_2 is the spin-relaxation time). The values of R are indicated on each curve. For the GIC plate investigated, L and δ are equal to the sample width (l) and the skin depth δ_c, respectively

The CESR measurements were carried out using an X-band E-line spectrometer in a rectangular cavity with TE_{102} mode. The constant magnetic field (H_0) modulation frequency and amplitude were 2.5 kHz and ~0.1 mT, respectively.

The effect of temperature on σ_a and σ_c was studied using plates of sizes $0.4 \times 0.4 \times 0.02$ and $0.04 \times 0.4 \times 0.02$ cm^3, respectively, at temperatures 77–300 K. The temperature was varied by regulating the rate and temperature of nitrogen gas flow through the quartz dewar with the sample. The temperature was maintained constant to within ~0.1 K/h and measured with an accuracy of ~0.5 K.

3. Results

Outside the interval of existence of an incommensurate phase of $C_{10}HNO_3$ σ_a and σ_c increase upon decreasing temperature (Fig. 2). As is seen from Fig. 2, at the liquid–solid phase transition both conductivities increase stepwise. Below T_c σ_a continues to increase monotonously, while a temperature dependence of σ_c is absent. The temperature dependence of σ_c is restored only below the "lock-in" phase transition temperature.

Over the entire temperature range of investigation the CESR spectrum of $C_{10}HNO_3$ consists of a single asymmetric line determined by Dyson mechanism [37]. The CESR spectrum is axial with respect to the c-axis and is characterized by $g_\parallel = 2.0023 \pm 0.0002$ and $g_\perp = 2.0028 \pm 0.0002$. At room temperature, the CESR linewidth is equal to $\Delta H_\parallel = (0.38 \pm 0.02) \times 10^{-4}$ T and $\Delta H_\perp = (0.36 \pm 0.02) \times 10^{-4}$ T. Here, $g_\parallel$ ($\Delta H_\parallel$) and $g_\perp$ ($\Delta H_\perp$) are values of the g-tensor (the linewidth) at H_0 being parallel and perpendicular to the c-axis, respectively. Down to $T_c \sim 250$ K, the width of the CESR line (measured at half of the height of peak A) does not depend on temperature. Upon intercalate crystallization, the linewidth undergoes a stepwise increase in of about three times. At microwave field power levels far from saturation and at the same temperature, the CESR linewidths in the Q and X-bands coincide, indicating that the line is homogeneously broadened. In both the

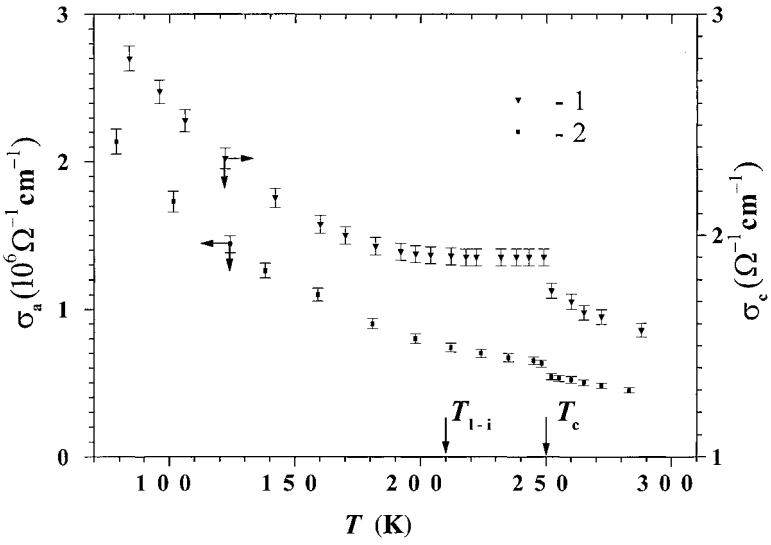

Fig. 2. Temperature dependences of (1) σ_c and (2) σ_a in $C_{10}HNO_3$. T_c and $T_{l\text{-}i}$ are the liquid–solid and the "lock-in" phase transition temperatures, respectively

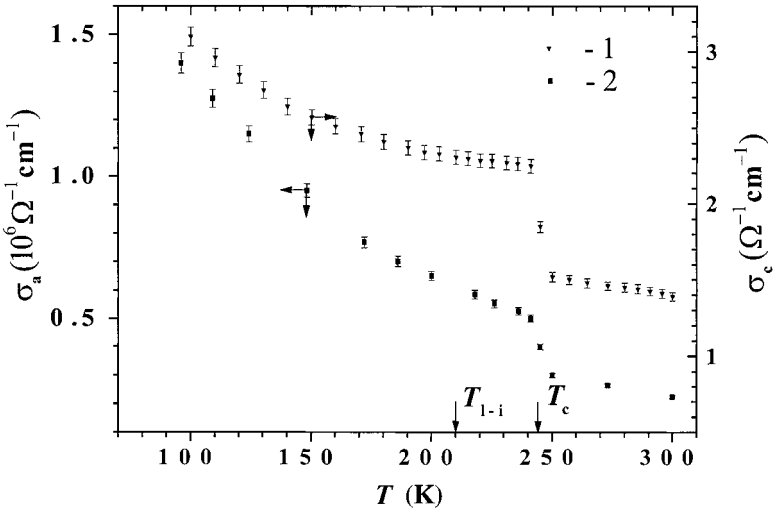

Fig. 3. Temperature dependences of (1) σ_c and (2) σ_a in $C_{15}HNO_3$. T_c and $T_{l\text{-}i}$ are the liquid–solid and the "lock-in" phase transition temperatures, respectively

liquid and crystal phases of the intercalate, the values of parameter $R_a = (T_{Da}/T_2)^{1/2}$ (T_{Da} is the in-plane spin diffusion time across the skin depth δ_c, and T_2 is the spin-relaxation time), which were determined using the experimental values of *A/B* for GIC plates with $l \gg \delta_c$ and well known Feher and Kip [40] nomograms, are practically independent of temperature. Upon intercalate crystallization, R_a undergoes a stepwise increase from ~1.8 up to ~3. The characteristics mentioned above of the temperature dependence of CESR lineshape parameters in the compounds investigated (with $l \sim 2\delta_c$) are qualitatively similar to those of wide plates $C_{10}HNO_3$ (with $l \gg \delta_c$) [32] studied before.

In $C_{15}HNO_3$ GICs the changes in σ_a and σ_c are qualitatively identical to those observed in the second stage compounds (Fig. 3). However, in this case the "plateau" in the temperature dependence of σ_c is a less marked one (Fig. 3).

For $C_{15}HNO_3$ GICs the CESR spectrum is axial with respect to the *c*-axis and is characterized by $g_\parallel = 2.0023 \pm 0.0002$, $g_\perp = 2.0028 \pm 0.0002$. At room temperature, the CESR line width is equal to $\Delta H_\parallel = (0.55 \pm 0.02) \times 10^{-4}$ T and $\Delta H_\perp = (0.58 \pm 0.02) \times 10^{-4}$ T. The CESR line is homogeneously broadened for all temperatures and upon intercalate crystallization, its width undergoes a stepwise increase by ~1.7 times [31]. In the GICs considered, as well as in the second stage compounds, the value of R_a practically does not depend on temperature both in the liquid and crystal phases of the intercalate. Upon the intercalate crystallization, it undergoes a stepwise increase from ~1.4 up to ~1.8. As for the second stage compounds, the characteristics mentioned above of the temperature dependence of CESR lineshape parameters in compounds investigated (with $l \sim 2\delta_c$) are qualitatively similar to those of wide plates $C_{15}HNO_3$ (with $l \gg \delta_c$) [31] studied before.

4. Discussion

Within the frameworks of non-band model of σ_c in acceptor GICs the charge transfer along the *c*-axis in compounds of large stage index (usually, for $n > 2$) may be realized

by essentially different mechanisms. The contributions of these mechanisms to σ_c depend on the nature of intercalate, stage of compounds, temperature and pressure [6, 15–20]. This is the reason why the magnitude and sign of the temperature coefficient of conductivity $d\sigma_c/dT$ for these compounds depends both on GIC structure and on external experimental conditions [6, 15–20]. In the case of the lowest stage compounds ($n = 1, 2$) the main contribution to σ_c is from the mechanism of charge transfer through the defect-mediated narrow high-conductivity paths (channels) [6, 15–20]. According to Sugihara and coworkers [19, 20] the value of this contribution to σ_c is described as

$$\sigma_c = \frac{16e^2}{\hbar^3}\, m^* d_I V_0^2 \left(\frac{N_c}{\Gamma}\right), \tag{1}$$

where V_0 is the matrix element of the scattering potential, N_c is the number of conduction paths per unit cell, m^* is the effective mass of carriers, d_I is the distance between nearest neighbour layers with an intervening intercalate layer, e is the electron charge, $\hbar$ is Planck's constant, and $\Gamma/\hbar$ is the sum of the relaxation rates due to phonon and impurity scattering: $\Gamma/\hbar = \Gamma_{ph}/\hbar + \Gamma_I/\hbar$. At high temperatures it is possible to consider $\Gamma/\hbar$ with good accuracy to be equal to the relaxation rate of current carriers in the graphite basal plane $\Gamma_a/\hbar$ associated with the σ_a [19, 20].

In the presence of coupling of the graphite bands across the intercalant, the tight-binding calculations of σ_c for low stage GICs lead to [10, 12],

$$\sigma_c \propto K \frac{e^2}{\pi\hbar^3}\, d_I \left(\frac{B^2}{\Gamma}\right), \tag{2}$$

where K includes both numerical and energy-related factors, B is the c-axis interaction energy or resonance integral linking graphite states separated by an intercalate layer, and other designations have the same sense as in Eq. (1). According to Markiewich [10, 12]

$$B = B_0 \exp\left(-d_I/d_0\right),$$

where $d_0 \cong 0.71$ Å.

Neglecting the temperature changes in d_I and V_0, from Eqs. (1) and (2) the conclusion follows that in GICs in some temperature interval σ_c can remain constant, in the presence of a temperature-dependent σ_a (and, hence, Γ ($\propto \Gamma_a$)), only if within this interval there is complete mutual compensation of temperature changes in Γ and B^2 (the band model) or in Γ and N_c (the conduction path model). Within the frameworks of the band model of σ_c in GICs, it is not possible to find the physically reasonable mechanism, which could provide the temperature changes in Γ and B required for the constancy of this conductivity. On the contrary, in the conduction path model of σ_c, it is possible to specify the reason why the ratio N_c/Γ (which determines this conductivity according to Eq. (1)) may be independent of temperature in some GIC phases. Such a reason may be a high concentration of defects N_d in these phases, when in a first approximation $\Gamma/\hbar$ is determined only by processes of scattering of current carriers on defects, i.e. $\Gamma/\hbar \cong \Gamma_I/\hbar \propto N_d$. If, furthermore, $N_c \propto N_d$, it is obvious, that in GIC phases with a high content of defects, the ratio N_c/Γ and, according to Eq. (1), σ_c may be independent of temperature. In such GIC phases, any change in N_d directly results in a change of σ_a. At the same time, a change in N_d can have an effect on σ_c only at its decrease and, moreover, this decrease should be so considerable that the contribution

of $\Gamma_{ph}/\hbar$ to $\Gamma/\hbar$ may not be neglected. Thus, it is possible to explain the absence of temperature dependence of σ_c in an incommensurate phase of $C_{10}HNO_3$, but with a temperature dependet σ_a, by the occurrence of new structural defects in a sample upon incommensurate crystallization of intercalate, whose concentration decreases as the temperature decreases. It is worth to noticing, that the significant CESR signal broadening (about three times) at the intercalant subsystem crystallization also indirectly confirms the point of view about more defective structure of $C_{10}HNO_3$ in its incommensurate phase.

It is known [41, 42] that in the modulated phases of crystals, alongside with the orientational domains, wide domain walls between the translational domains ("stripe domains") and structural solitons can occur. As the "lock-in" transition temperature is approached, the concentration of these structural imperfections decreases. According to X-ray data [29], similar structural imperfections can be present in $C_{10}HNO_3$ below the intercalant crystallization temperature. The research data by the method of quasi-elastic neutron scattering of $C_{10}HNO_3$ [30] confirm this conclusion and, testify the decrease of the "stripe domain" concentration, as the "lock-in" transition temperature is approached. Hence, if in an incommensurate phase of $C_{10}HNO_3$, $\Gamma_{ph}/\hbar \gg \Gamma_l/\hbar$ and some high-conductivity paths (channels) are formed at intercalate crystallization, caused by "stripe domains" or structural solitons in intercalate layers, then the decrease of their concentration upon approaching to the "lock-in" — transition temperature can result in a σ_a increase, which can occur at a constant value of σ_c. From the above considerations it follows also, that in some phases of GICs, the "metallic" temperature dependence of σ_a can be determined not by the decrease in amplitudes of thermal oscillations of atoms in carbon and intercalate layers, but due to the in-plane intercalant structural ordering.

In the framework of the above model of σ_c in the incommensurate phase of $C_{10}HNO_3$, the non-zero value of $|d\sigma_c/dT|$ in incommensurate phase of $C_{15}HNO_3$ (Fig. 3) may be easily explained taking into account that in the latter the concentration of defects due to intercalate crystallization is less than in the former and, therefore, the conduction electron relaxation rate due to phonon scattering is not negligible. The decrease of concentration of defects originating from intercalate crystallization in $C_{15}HNO_3$ is indirectly proved by the smaller increase in CESR linewidth upon intercalate crystallization in these compounds than in second stage ones.

Crystallization of the intercalate subsystem in the GICs investigated also initiates the change of its electronic structure [43], which, in particular, results in an increase of the electron-state density on the Fermi surface [44]. This allows interpreting the stepwise increase of σ_a upon intercalate crystallization in $C_{5n}HNO_3$ ($n = 2, 3$) (Figs. 2 and 3), as caused by the stepwise increase of current carrier concentration. The conductivity increase due to this factor exceeds its expected decrease caused by the decrease of current carrier mobility (due to the increase of concentration of structural defects).

In the literature, the problem of searching for and analysing of possible anomalous features of electrical conductivity in incommensurate phases of GICs has not been considered. At the same time, our analysis of the literature has shown, that among GICs for which the temperature dependence of σ_c was studied, there are some compounds with incommensurate phases. They are acceptor GICs of third, fourth and sixth stages with $SbCl_5$ [45], in which the intercalate subsystem at $T \approx 210$ K undergoes a phase transition into the incommensurate phase [46]. In all these GICs the absolute value of temperature coefficient of σ_a decreases at the incommensurate phase transition and it remains small (in compounds of third and fourth stages it is absent in fact) in a broad

temperature range ($\Delta T \approx 100$ K) below the phase transition temperature. These facts allow us to suppose that the temperature invariability of σ_c revealed by us in an incommensurate phase of $C_{10}HNO_3$ can be a characteristic feature of all low-stage structural incommensurate phases of acceptor GICs.

In summary, with using Eq. (1) we can estimate the concentration of narrow highly conductive channels along the *c*-axis between graphite layers through the intervening intercalate layers in an incommensurate phase of $C_{10}HNO_3$ immediately after crystallization of the intercalate. For this purpose we shall neglect the possible difference of $\Gamma/\hbar$ from $\Gamma_a/\hbar$ and we believe, that the latter can be determined from the Drude expression: $\sigma_a = Ne^2/(\Gamma_a/\hbar)\, m^*$ (N is the concentration of current carriers). Then, inserting in Eq. (1) the following set of parameters: σ_c =1.9 $\Omega^{-1}\,cm^{-1}$, $\sigma_a = 8 \times 10^5\ \Omega^{-1}\,cm^{-1}$, $V_0 = (2\text{–}3) \times 10^{-2}$ eV [11, 13, 14], $N = 1.02 \times 10^{21}\ cm^{-3}$ [47] $d_I = 7.80$ Å and $m^* = (0.06\text{–}0.32)m_0$ [48–53] (m_0 being the mass of free electron), we have found: $N_C = (1.1\text{–}65) \times 10^{-5}$ paths/unit cell. (Values of σ_c, σ_a and d_I, utilized in calculation of N_C, have been determined by us. The values of V_0 and m^* for GICs with nitric acid are not known. Therefore, at estimation of N_I, known from literature minimum and maximum values of these parameters in other acceptor GICs was used). It is worth noticing that according to an estimation of Suzuki et al. [20], in second stage GICs with $MoCl_5$ $N_C \sim 5 \times 10^{-5}$ paths/unit cell. As may be seen, despite the different nature of these intercalates, the value of N_i for the latter GICs is within the interval of its estimated values in an incommensurate phase of $C_{10}HNO_3$.

5. Conclusion

In this work, we have presented contactless conductivity and CESR measurement data for the GICs $C_{5n}HNO_3$ with $n = 2$ and 3. Outside the interval of existence of an incommensurate phase of these compounds, both σ_a and σ_c increase upon decreasing the temperature. In the incommensurate phase of the second stage compounds, the temperature dependence of σ_c is absent, in spite of preservation of a "metallic" temperature dependence of σ_a. In the third stage compounds the similar "plateau" is a less marked one. In both stages of GICs investigated, at the incommensurate crystallization of the intercalate subsystem, the CESR linewidth undergoes a stepwise increase. We have shown that experimental conductivity data may be explained within the framework of a model, based on the transport of free charge carriers along the *c*-axis through the defect-mediated narrow high-conductivity paths (channels).

Acknowledgements The author is grateful to N. M. Mishchenko and V. V. Sereda for help in experiments, to L. B. Nepomnyashchii (Scientific Research Centre for Graphite, Moscow) for providing the HOPG samples and to Prof. K. Sugihara (Japan, Nihon University) for useful comments. This work was supported by the Russian Foundation for Basic Research (grant No. 00-03-32610).

References

[1] M. S. DRESSELHAUS and G. DRESSELHAUS, Adv. Phys. **30**, 139 (1981).
[2] S. A. SOLIN and H. ZABEL, Adv. Phys. **37**, 87 (1988).
[3] G. M. T. FOLEY, C. ZELLER, E. R. FALARDEAU, and F. L. VOGEL, Solid State Commun. **24**, 371 (1977).
[4] A. R. UBBELOHDE, Proc. R. Soc. Lond. A **327**, 289 (1972).

[5] A. R. Ubbelohde, Synth. Met. **1**, 13 (1979/1980).
[6] D. T. Morelli and C. Uher, Phys. Rev. B **27**, 2477 (1983).
[7] E. McRae and J. F. Mareche, J. Mater. Res. **3**, 75 (1988).
[8] A. F. Ioffe and A. R. Regel, Prog. Semicond. **4**, 237 (1960).
[9] N. F. Mott, Electronic and Structural Properties of Amorphous Semiconductors, Eds. P. G. Le Comber and J. Mort, Academic Press, London 1973 (p. 1).
[10] R. S. Markiewicz, Solid State Commun. **57**, 237 (1986).
[11] H. Zaleski and W. R. Datars, Phys. Rev. B **35**, 7690 (1987).
[12] R. S. Markiewicz, Phys. Rev. B **37**, 6453 (1988).
[13] E. McRae, J. F. Mareche, P. Pernot, and R. Vangelisti, Phys. Rev. B **39**, 9922 (1989).
[14] E. McRae, O. E. Andersson, M. Lelaurain, V. Polo, B. Sundqvist, and R. Vangelisti, J. Phys. Chem. Solids **57**, 827 (1996).
[15] K. Sugihara, Phys. Rev. B **29**, 5872 (1984).
[16] S. Shimamura, Synth. Met. **12**, 365 (1985).
[17] K. Sugihara, Phys. Rev. B **37**, 4752 (1988).
[18] K. Matsubara, K. Sugihara, and T. Tsuzuku, Phys. Rev. B **41**, 969 (1990).
[19] K. Sugihara, J. Phys. Soc. Jpn. **62**, 624 (1993).
[20] M. Suzuki, C. Lee, I. S. Suzuki, K. Matsubara, and K. Sugihara, Phys. Rev. B **54**, 17128 (1996).
[21] M. Bottomley, G. S. Parry, and A. R. Ubbelohde, Proc. R. Soc. Lond. A **279**, 291 (1964).
[22] D. E. Nixon, G. S. Parry, and A. R. Ubbelohde, Proc. R. Soc. Lond. A **291**, 324 (1966).
[23] A. R. Ubbelohde, Carbon **6**, 177 (1966).
[24] A. R. Ubellohde, Proc. R. Soc. Lond. A **304**, 25 (1968).
[25] K. Kawamura, T. Saito, and T. Tsuzuku, Carbon **13**, 452 (1975).
[26] A. Avagadro and M. Villa, J. Chem. Phys. **66**, 2359 (1977).
[27] S. K. Khanna, E. R. Falardeau, A. J. Heeger, and J. E. Fischer, Solid State Commun. **25**, 1059 (1978).
[28] A. Dvorkin and A. R. Ubbelohde, Carbon **16**, 291 (1978).
[29] E. J. Samuelson, R. Moret, H. Fuzellier, M. Klatt, M. Lelaurain, and A. Herold, Phys. Rev. B **32**, 417 (1985).
[30] F. Batallan, I. Rosenman, A. Magerl, and H. Fuzellier, Phys. Rev. B **32**, 4810 (1985).
[31] A. M. Ziatdinov and N. M. Mishchenko, Solid State Commun. **97**, 1085 (1996).
[32] A. M. Ziatdinov and N. M. Mishchenko, Modern Applications of EPR/ESR: From Biophysics to Material Science, Ed. C. Rudowicz, Springer-Verlag, Berlin/Heidelberg/New York 1998 (pp. 562–570).
[33] A. M. Ziatdinov and N. M. Mishchenko, J. Phys. Chem. Solids **58**, 1161 (1997).
[34] L. A. Pendrys, C. Zeller, and F. L. Vogel, J. Mater. Sci. **15**, 2103 (1980).
[35] M. Saint Jean and E. McRae, Phys. Rev. B **43**, 3969 (1991).
[36] H. Kodera, J. Phys. Soc. Jpn. **28**, 89 (1970).
[37] F. J. Dyson, Phys. Rev. **98**, 349 (1955).
[38] A. M. Ziatdinov and N. M. Mishchenko, Phys. Solid State (Russia) **36**, 1283 (1994).
[39] J. Blinowski, P. Kacman, C. Rigaux, and M. Saint-Jean, Synth. Met. **12**, 419 (1985).
[40] G. Feher and A. F. Kip, Phys. Rev. **93**, 337 (1955).
[41] A. D. Bruce and R. A. Cowley, J. Phys. C **11**, 3577 (1978).
[42] P. Bak, Rep. Prog. Phys. **45**, 587 (1982).
[43] A. M. Ziatdinov and Yu. M. Nikolenko, Phys. Solid State (Russia) **35**, 2259 (1993).
[44] A. M. Ziatdinov and N. M. Mishchenko, Science and Technology of Carbon, Ext. Abstracts, Vol. 1, ed. Eurocarbon Group, Strasbourg (France), July 1998 (p. 775).
[45] C. Uher and D. T. Morelli, Mater. Res. Soc. **20**, 163 (1983).
[46] H. Homma and R. Clarke, Phys. Rev. B **31**, 5865 (1985).
[47] F. L. Vogel, H. Fuzellier, C. Zeller, and E. J. McRae, Carbon **17**, 255 (1979).
[48] E. Mendez, T. C. Chieu, N. Kambe, and M. S. Dresselhaus, Solid State Commun. **33**, 837 (1980).
[49] W. R. Datars, P. K. Ummat, H. Aoki, and S. Uji. Phys. Rev. B **48**, 18174 (1993).
[50] V. A. Kulbachinskii, S. G. Ionov, S. A. Lapin, V. V. Avdeev, E. A. Kamenskaya, and A. De Visser, Mol. Cryst. Liq. Cryst. **245**, 31 (1994).
[51] V. A. Kulbachinskii, S. G. Ionov, S. A. Lapin, and V. V. Avdeev. J. Phys. I (France) **2**, 1941 (1992).
[52] G. Wang, P. K. Ummat, and W. R. Datars, Phys. Rev. B **47**, 3864 (1993).
[53] T. R. Chien, D. Marchesan, P. K. Ummat, and W. R. Datars, J. Phys.: Condens. Matter **6**, 3031 (1994).